Pharmacodynamic and Response Biomarkers in the Monotherapy Arm of a Phase 1 Trial of CTX-471, a Novel Anti-CD137 Agonist Antibody

Kris Sachsenmeier, Niharika Mettu, Martin Gutierrez, Jeffery Edenfeld, Seth Rosen, Minal Barve, Karin Herrera, Natalie Warholic, Diana Albu, Alberto Visintin, Thomas Schuetz, Tanner Johanns

Compass Therapeutics Inc. | 80 Guest Street | Boston MA 02135 | USA

INTRODUCTION

- Cancer therapy has been transformed by immune checkpoint inhibition with antibodies targeting programmed cell death 1 (PD-1) and programmed cell death ligand 1 (PD-L1). Yet response is limited in a significant proportion of patients who either do not respond to or progress following an initial response to these treatments. There is a clear need for novel immunotherapies.
- Development of agonist antibodies targeting activating receptors has been a challenge. A key costimulatory receptor on activated T and NK cells is CD137 (4-1BB) but a number of drugs in development targeting CD137 have been limited by hepatic toxicity.
- CTX-471 is a unique antibody agonist of CD137 and has been characterized in preclinical studies[1,2]. The antibody binds to a unique epitope and intermediate affinity antibodies were shown to be optimal in preclinical efficacy studies.
- CTX-471-001 is a phase 1 study that evaluated the safety and tolerability of CTX-471 in patients who had previously received a PD-1 or PD-L1-containing regimen.
- This report presents exploratory data for pharmacodynamic and response biomarker analyses of the escalation and expansion cohorts and complements safety and efficacy published at ASCO 2024[3].
- Clinical Trial information: NCT03881488, Research Sponsor: Compass Therapeutics, Inc.

METHODS

Tissue and blood were taken at baseline and prior to dosing on week 9 of CTX-471 alone. The 9-week timepoint was chosen to coincide with a CT scan. Samples were analyzed by multi-parameter immunofluorescence, flow cytometry, or a panel of cytokines using the Neogenomics Multi-omyx platform. Standard lab chemistry and blood cell counts were measured at each site. Tissue samples included diagnostic samples as well as a number of paired on-treatment biopsies. Correlates measured are listed in Table 1. For immunofluorescence, tumor vs non-tumor locations were identified using a tumor-specific counterstain of either pan-cytokeratin or SOX10 (melanoma) as appropriate. Staining of immune cells was confirmed by staining with anti-CD45.

To measure pharmacodynamic effects, comparisons made between pre- and post-CTX-471 treatment (pharmacodynamics). To survey response biomarkers, values from samples obtained from patients with tumors showing complete (CR) or partial responses (PR) as well as stable disease (SD) were compared with tumors showing progressive disease. Pharmacodynamic analyses used samples from all available indications. Response correlate analysis was restricted to indications for which at least four patients with evaluable samples were available. Using GraphPad Prism software, paired T-tests were performed for pharmacodynamics comparisons. For response biomarkers of baseline samples, an unpaired t-test was performed using Welch's correction when variance between samples could not be assumed. Asterisks indicate differences significant at either p=0.05 (*) or p=0.01(**).

Table1. Tissue and Blood Correlates Measured for Exploratory Analysis

ALLCELLS #	CD8+ #per mmsq	CD3+CD4+LAG3+	plat
CD137+ #	FOXP3+ #per mmsq	CD3+CD4+PD-1+	hct
CD3+ #	KI67+ #per mmsq	CD3+CD4+PD-L1+	mcv
CD3DB+ #	PD1+ #per mmsq	CD3+CD4+TIGIT+	baso
CD4+ #	PDL1+ #per mmsq	CD3-CD56brCD16dim CD137+	eos
CD45+ #	TUMOR+ #per mmsq	CD3-CD56brCD16dimNKp30+	lym
CD56+ #	CD3+CD4+ #per mmsq	CD3-CD56brCD16dim NK	mono
CD64+ #	CD3+CD8+ #per mmsq	CD3-CD56brCD16dimNKG2D+	neut
CD8+ #	CD3+CD137+ #per mmsq	CD3-CD56brCD16dimTIGIT+	baso_per
FOXP3+ #	CD3+CD4+CD137+ #per mmsq	CD3-CD56dimCD16+CD137+	eos_per
KI67+ #	CD3+CD8+CD137+ #per mmsq	CD3-CD56dimCD16+NKp30+	lym_per
PD1+ #	CD3+CD4+PD1+ #per mmsq	CD3-CD56dimCD16+ NK	mono_per
PDL1+ #	CD3+CD8+PD1+ #per mmsq	CD3-CD56dimCD16+NKG2D+	neut_per
TUMOR+ #	CD3+CD4+PDL1+ #per mmsq	CD3-CD56dimCD16+TIGIT+	sodium
CD3+CD4+ #	CD3+CD45+CD56+ #per mmsq	CD3+CD8+CCR7+CD45RA+	k
CD3+CD8+ #	CD137+FOXP3+ #per mmsq	CD3+CD8+CCR7-CD45RA-	crp
CD3+CD137+ #	CD45+CD56+CD137+ #per mmsq	CD3+CD8+CCR7-CD45RA+	phos
CD3+CD4+CD137+ #	CD45+CD56+PD1+ #per mmsq	CD3+CD8+CCR7+CD45RA+	ca
CD3+CD8+CD137+ #	CD3+PDL1+ #per mmsq	CD3+CD8+CD137 (4-1BB)+	mg
CD3+CD4+PD1+ #	CD3+CD8+PDL1+ #per mmsq	CD3+CD8+CD25+	bicarb
CD3+CD8+PD1+ #	CD3+KI67+ #per mmsq	CD3+CD8+KI67+	bun
CD137+PD1+ #	CD3+CD4+KI67+ #per mmsq	CD3+CD8+LAG3+	amy
CD3+CD4+CD56+ #	CD3+CD8+KI67+ #per mmsq	CD3+CD8+PD-1+	lip
CD137+FOXP3+ #	PD1+PDL1+ #per mmsq	CD3+CD8+PD-L1+	gluc
CD45+CD56+CD137+ #	CD32B+CD64+ #per mmsq	CD3+CD8+TIGIT+	alb
CD45+CD56+PD1+ #	CD137+KI67+ #per mmsq	Cytotoxic T-cells CD3+CD8+	bili
CD3+PDL1+ #	TUMOR+KI67+ #per mmsq	Helper T-cells CD3+CD4+	ast
CD3+CD8+PDL1+ #	TUMOR+PDL1+ #per mmsq	Lymphocytes	alt
CD3+KI67+ #	TUMOR+CD137+ #per mmsq	T-cells CD3+	alp
CD3+CD4+KI67+ #	CD14+ Monocytes	CD3+CD4+CD25+CD127low	
CD3+CD8+KI67+ #	CD3-CD19+ B-cells	CD3+CD4+ (non T-reg)	
PD1+PDL1+ #	CD3+CD4+CCR7+CD45RA+	CD3+CD56brightCD16dim CD137 (4-1BB)+	
CD32B+CD64+ #	CD3+CD4+CCR7+CD45RA-	CD3-CD56brightCD16dim NK-cells	
CD137+KI67+ #	CD3+CD4+CCR7-CD45RA-	CD3-CD56dimCD16+CD137 (4-1BB)+	
TUMOR+KI67+ #	CD3+CD4+CCR7-CD45RA+	CD3-CD56dimCD16+ NK-cells	
TUMOR+PDL1+ #	CD3+CD4+CD137 (4-1BB)+	ccl2_je_mcp1	
TUMOR+CD137+ #	CD3+CD4+CD25+	cxcl10_ip10_crg2	
ALLCELLS #per mmsq	CD3+CD4+CD25+FoxP3+CD137+	cxcl9_mig	
CD137+ #per mmsq	CD3+CD4+CD25+FoxP3+KI67+	il10	
CD3+ #per mmsq	CD3+CD4+CD25+FoxP3+LAG3+	il6	
CD32B+ #per mmsq	CD3+CD4+CD25+FoxP3+PD-1+	il8_cxcl8	
CD4+ #per mmsq	CD3+CD4+CD25+FoxP3+PDL1+	tnf_alpha	
CD45+ #per mmsq	CD3+CD4+CD25+FoxP3+TIGIT+	rbc	
CD56+ #per mmsq	CD3+CD4+CD25+FoxP3+ Treg	hgb	
CD64+ #per mmsq	CD3+CD4+KI67+		

Tissue Immunofluorescence
Flow Cytometry
Cytokines
Hematology
Lab Chemistry

CONCLUSIONS

CTX-471 showed pharmacodynamic biomarkers indicating immune stimulation. Examples include increases in both CD4 and CD8 T cells expressing CD137 (Figure 1, Panels B & C) as well as NKp30 positive NK cells (Panel E). Tumor tissue showed elevated levels of both PD-1 and PD-L1 (Panel D). Paired images of pre- and post-CTX-471 treated tissue showed an increase in PD-L1 staining (Panel F).

CTX-471 disease control is associated with measurable baseline biomarkers. An interesting trend was observed when comparing tissue with circulating correlates. For example, total tissue NCAM (CD56) positive cell density (Figure 2, Panel B) as well as activated NK cells (Figure 2, Panels G & H) showed significantly higher levels at baseline in disease control samples when compared with samples taken from patients eventually showing progressive disease. In contrast, circulating NK cells (Figure 2, Panels J & K), whether differentiated ("CD56dim") or not ("CD56bright") were significantly lower at baseline in disease control patient samples.

Baseline tumor cell expression of NCAM/CD56 is associated with disease control. A strikingly different pattern and intensity of immunofluorescent NCAM (CD56) signal was observed in Figure 3 comparing samples from patients that did (Figure 3, Panels A-C) or did not (Figure 3, Panels D-F) show disease control. This observation is consistent with previous reports[4,5] for trans-homotypic interactions between NCAM on different cells and the functional impact of those interactions[6,7]. Such interactions could form a mechanistic basis for superior response to CTX-471 in tumors expressing high levels of NCAM. i.e., homotypic interactions between tumor cells and NCAM positive effector cells could promote tumor localization of cells such as NK cells which have been shown[1] to be required for killing of tumor cells by CTX-471 preclinically. Baseline tumor samples were classified as "high" or "low" using the median CD56 positive cells/mm^2. High NCAM tumors were enriched for activated (CD137$^+$) NK cells but not for lymphocytes which typically do not express NCAM such as CD8 and CD4 T cells (Panel C). A mechanism by which NCAM-expressing tumors might enrich for CD137-expressing NK cells and thus for CTX-471 response is proposed in Panel D.

A novel baseline circulating cell phenotype identifies partial response to CTX-471. A novel phenotype-agnostic and computationally-based approach to analyzing conventional flow cytometry data was used (Figure 4). A specific subset of cells that were CD14$^+$CD11b$^+$ and CD56$^+$ prior to CTX-471 treatment was validated with a set of samples analyzed separately from a Discovery Set of samples used to identify the phenotype. This phenotype would likely have been overlooked using conventional human-based flow cytometry analysis.

A Phase 2 study of CTX-471 in patients with NCAM$^+$ tumors is planned.

Figure 1. CTX-471 Monotherapy Shows Pharmacodynamic Correlates of Tumor Immunity

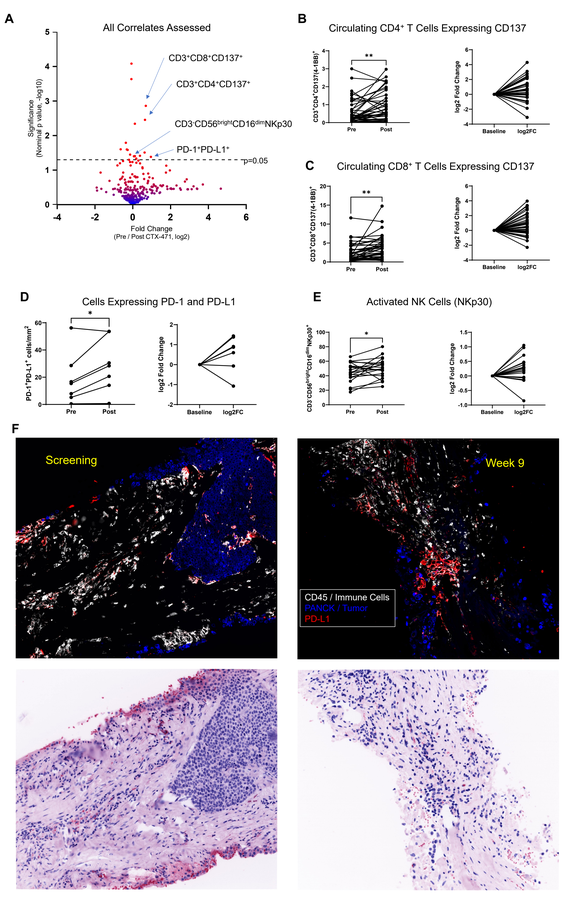

Figure 1. Paired pre- and post-CTX-471 treatment tumor and blood samples were analyzed using multiplexed immunofluorescence and by flow cytometry. A summary of all pharmacodynamic correlates measured and listed in Table 1 is seen in a volcano plot (Panel A) with those showing a nominal p value of lower than p=0.05 indicated with the horizontal dashed line. In the remaining panels, the raw and fold-change values of the indicated correlates are plotted. In Panel F, levels of PD-L1 on tumor tissue were observed to increase following treatment. The lower two panels are the respective H&E images from panels immediately above. Asterisks indicate differences significant at either p=0.05 (*) or p=0.01(**).

Figure 2. Biomarker Correlates Linked with Disease Control On CTX-471 Monotherapy

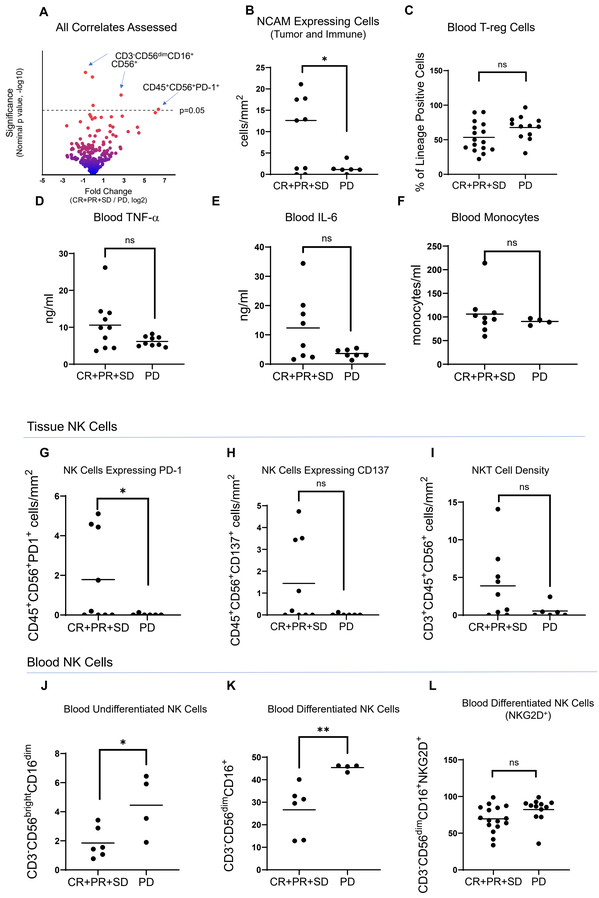

Figure 2. Tumor and blood samples taken at baseline and compared between patients with tumors showing disease control (CR, PR, and SD) or progressive disease (PD). A summary of all response biomarkers measured as listed in Table 1 is seen in a volcano plot (Panel A) with those showing a nominal p value of lower than p=0.05 indicated by a horizontal dashed line. An antibody to CD56 / NCAM was included within the multiplexed immunofluorescent panel in order to detect NK cells. However, in addition to NK cell staining, a surprisingly high staining in tumor cells was observed to be associated with disease control (Panel B). Other baseline phenotypes of interest included blood cytokines TNFα and IL-6, monocytes per ml of blood and regulatory T cells. A focused survey of NK subsets was made within tumor (Panels G–I) and blood (Panels J–L) samples. Subsets measured in tissue included activated NK (Panels G & H), as well as NKT cells (Panel I). Circulating NK cells (Panels J-L) also showed significant differences and trends with disease control in baseline samples. Asterisks indicate differences significant at either p=0.05 (*) or p=0.01(**).

Figure 3. Tumor Cell NCAM / CD56 Staining Is Linked with Disease Control

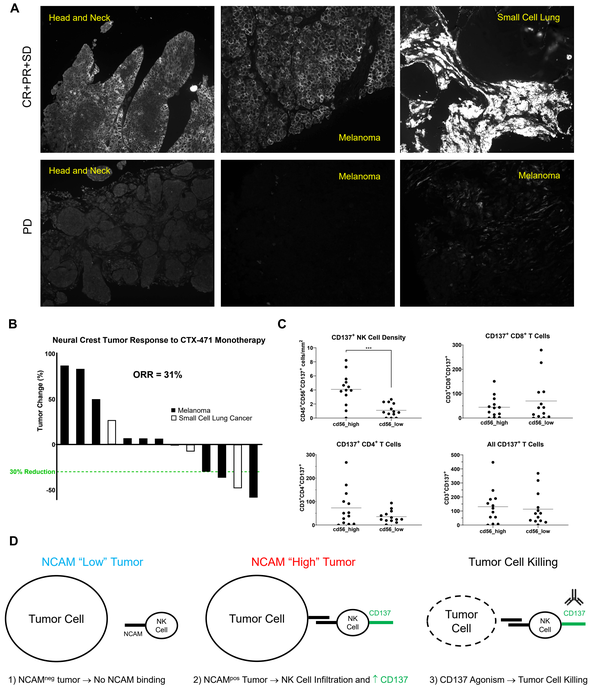

Figure 3. An immunofluorescent stain for NCAM intended to detect NK cells showed a clear "cobblestone" epithelial pattern on tumor cells of the tumor types shown (Panel A). This pattern was strongest in baseline samples from tumor showing disease control. In samples taken from matching tumor types showing progressive disease (e.g., melanoma or head and neck tumors), the NCAM staining pattern was relatively faint. In Panel B, a waterfall plot shows the best change in tumor size within tumors derived from the neural crest: small cell lung cancer and melanoma. Within this subset an overall response rate of 31% was achieved. Data in Panel C compares the densities of activated (CD137$^+$) cells for various lymphocyte subsets within all baseline tumor samples classified as high or low NCAM based upon median CD56 cell density. Panel D shows a proposed mechanism by which NCAM may render tumors sensitive to CTX-471 treatment. Asterisks indicate differences significant at p=0.001(***).

Figure 4: A Novel Baseline Circulating Biomarker of CTX-471 Response

Ozette Discovery™: Computationally Profiles the Entire Phenotype Space

- Comprehensive, high-resolution discovery of cellular phenotypes in single-cell cytometry datasets
- State of the art machine-learning for rapid, unbiased, reproducible and interpretable results
- Delivers fully annotated data that can be modeled to answer scientific questions and surface relevant cell populations
- Explore associations between phenotypes and metadata of interest in the Discovery dashboard

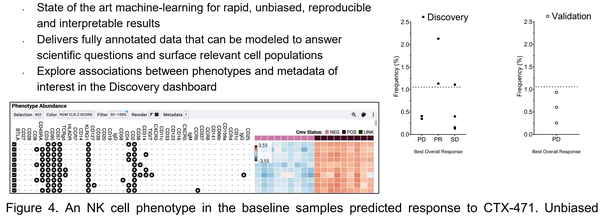

Figure 4. An NK cell phenotype in the baseline samples predicted response to CTX-471. Unbiased analysis of NK cell-focused flow cytometry panel was conducted using the Ozette Discovery Platform™ for full annotation of all robust cellular phenotypes. Ozette Discovery identified an NK cell phenotype: **CD16$^+$CD11b$^+$CD56$^+$CD3$^-$CD19$^-$CD314$^-$CD337$^-$TIGIT$^-$CD137$^-$** which clearly distinguished melanoma patients with disease control from those showing progressive disease. For example, a threshold of 1% as indicated by the dotted lines would classify PR patient samples as distinct from PD and most SD samples. This unique phenotype went undetected using conventional analytical approaches and highlights the importance of leveraging the full extent of the data and an unbiased discovery approach.

REFERENCES

1. Eskiocak U, Guzman W, Wolf B, et al. Differentiated agonistic antibody targeting CD137 eradicates large tumors without hepatotoxicity. *JCI Insight*. 2020;5(5):e133647, 133647. doi:10.1172/jci.insight.133647
2. Eskiocak U, Guzman W, Zizlsperger N, et al. CTX-471, a novel agonistic antibody targeting CD137, eradicates very large tumors by selectively reprogramming the tumor microenvironment without causing hepatic toxicity. In: *33rd Annual Meeting & Pre-Conference Programs of the Society for Immunotherapy of Cancer (SITC 2018)*. Vol P407. Society for Immunotherapy of Cancer; 2018. https://jitc.biomedcentral.com/articles/10.1186/s40425-018-0423-x#Sec1
3. Barve MA, Johanns TM, Mettu NB, et al. Phase 1 study of CTX-471, a novel CD137 agonist antibody, in patients with progressive disease following PD-1/PD-L1 inhibitors in metastatic or locally advanced malignancies. *J Clin Oncol*. 2024;42(16_suppl):2535-2535. doi:10.1200/JCO.2024.42.16_suppl.2535
4. Gunesch JT, Dixon AL, Ebrahim TA, et al. CD56 regulates human NK cell cytotoxicity through Pyk2. *eLife*. 2020;9:e57346. doi:10.7554/eLife.57346
5. Van Acker HH, Van Acker ZP, Versteven M, et al. CD56 Homodimerization and Participation in Anti-Tumor Immune Effector Cell Functioning: A Role for Interleukin-15. *Cancers*. 2019;11(7):1029. doi:10.3390/cancers11071029
6. Taouk G, Hussein O, Zekak M, et al. CD56 expression in breast cancer induces sensitivity to natural killer-mediated cytotoxicity by enhancing the formation of cytotoxic immunological synapse. *Sci Rep*. 2019;9(1):8756. doi:10.1038/s41598-019-45377-8
7. Valgardsdottir R, Capitanio C, Texido G, et al. Direct involvement of CD56 in cytokine-induced killer–mediated lysis of CD56+ hematopoietic target cells. *Exp Hematol*. 2014;42(12):1013-1021.e1. doi:10.1016/j.exphem.2014.08.005

SITC 2024, November, Houston, USA & Online

ACKNOWLEDGEMENTS

The authors express their appreciation to Nicole Gampp for exceptional editorial assistance, and to the Compass leadership team for their steadfast support. Gratitude is also extended to the numerous unnamed individuals within the company and at the clinical sites whose contributions were integral to the success of this project.